Development of the Vortex Mass Flowmeter with Wall Pressure Measurement

Zhiyong Li[1,2], Zhiqiang Sun[1,2]

[1]School of Energy Science and Engineering, Central South University, Changsha 410083, China
[2]Hunan Key Laboratory of Energy Conservation in Process Industry, Central South University, Changsha 410083, China
e-mail: zqsun@csu.edu.cn

Mass flow measurement is essential to the understanding and control of processes concerning fluid flow. The availability of reliable mass flowmeters, however, is far inadequate to meet the demand. In this paper we developed a practical vortex mass flowmeter with wall pressure measurement. The meter coefficient of mass flow rate was acquired through experiments with air at Reynolds numbers from 1.3×10^3 to 9.8×10^3. Here we show that the meter coefficient of mass flow rate is nearly constant at Reynolds numbers greater than 5.5×10^3. To further extend the lower limit, a correction factor related to the Reynolds number was introduced into the vortex mass flowmeter. The results show that the relative errors of the vortex mass flowmeter developed are basically within ±5%. This device can satisfy a diversity of requirements of mass flow measurement in engineering fields.

Keywords: Mass flow measurement, vortex mass flowmeter, vortex shedding, wall pressure, meter coefficient of mass flow rate, correction factor

1. INTRODUCTION

THE MEASUREMENT of mass flow rate has become a basic requirement in many commercial transactions involving conveyance of fluids over the last two decades [1]. This is partly due to the increasing value of products [2], but it is also due to an increasing realization that volumetric flow measurement is often inappropriate [3], [4]. However, so far the availability of mass flowmeters is much too inadequate to meet the demand.

Mass flow measurement is generally categorized as direct or indirect. Direct mass flow measurement with a single instrument is rare. Heretofore the approaches to direct mass flow rate are achieved by measuring Coriolis acceleration, or angular momentum, or temperature rise resulting from heat addition [5], [6]. In engineering applications, indirect mass flow measurement is widely accepted because of its simple installation and low maintenance. It is apparent that mass flow rate can be obtained by multiplying volumetric flow rate by fluid density. Moreover, indirect mass flow rate can also be accomplished by properly manipulating output signals from multiple sensors [7]. The major disadvantage of indirect mass flow measurement is the need for a suitable compensating algorithm. Thereby developing reliable mass flowmeters is of essential interest to the flow measurement community.

Since its introduction in the late 1960s, vortex flowmeter has been recognized as a promising flowmetering device and is widely accepted to measure the flow rate of gas, liquid, or even some multiphase flows [8]. The measurement principle of vortex flowmeter is based on the phenomenon of Kármán vortex street, in which the frequency of vortex shedding is proportional to the average fluid flow velocity [9], [10]. Due to its insensitiveness to most parameters of the fluid including density, temperature, and pressure, the vortex flowmeter is considered as a potential solution to mass flow measurement. The first attempt of using a vortex flowmeter to obtain mass flow rate was made by Itoh and Ohki [11]. They divided the lift force acting on the vortex shedder by the vortex shedding frequency, and yielded a signal that was proportional to the mass flow rate. Zhang *et al.* extracted the vortex shedding frequency and the pressure drop across a bluff body from the wall pressure difference by a single sensor, and related the mass flow rate directly to the quotient of pressure drop divided by vortex shedding frequency [12]. Sun achieved the measurement of mass flow rate of homogeneous gas-liquid bubble flow with combined use of a Venturi tube and a vortex flowmeter [13]. These investigations establish, in principle, the basis of mass flow measurement using a vortex flowmeter. According to the authors' knowledge, however, studies concerning the design of vortex mass flowmeter devices have not been reported in the literature.

This paper is aimed at developing a prototype vortex mass flowmeter of use value. Measurement performance of the vortex mass flowmeter is tested in a bell prover calibration system at Reynolds numbers from 1.3×10^3 to 9.8×10^3. Meter coefficients of mass flow rate are acquired by experiments. A correlation for determining appropriate correction factor at low Reynolds numbers is established. Finally, the measurement errors of the developed vortex mass flowmeter are analyzed and discussed.

2. PRINCIPLES & METHODOLOGY

A. Mass flow measurement based on vortex shedding

If two tappings are placed upstream and downstream of a bluff body, as shown in Fig.1, the detected wall pressure difference contains both fluid oscillation and pressure drop caused by the vortex shedding. From the fluctuation of the wall pressure difference, we can extract the vortex shedding frequency:

$$f = St \frac{U}{md}$$ (1)

$$m = 1 - \frac{2}{\pi}\left[\frac{d}{D}\sqrt{1-\left(\frac{d}{D}\right)^2} + \arcsin\frac{d}{D}\right] \quad (2)$$

where St represents the dimensionless Strouhal number, U is the average fluid flow velocity, m is the area ratio, d is the width of the bluff body, and D is the inner diameter of the flow passage.
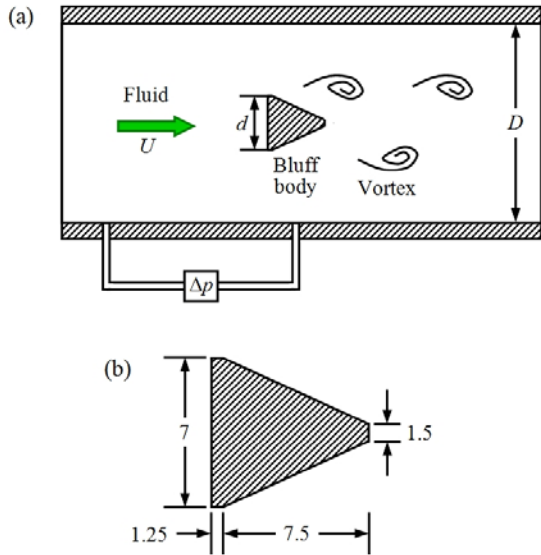

Fig.1. Schematic diagram of vortex mass flowmeter: (a) Overall structure; (b) Dimensions of bluff body (unit: mm).

Meanwhile, the average pressure difference represents the pressure drop and can be written as

$$\Delta\bar{p} = \frac{1}{2}C_{\mathrm{p}}\rho U^2 \quad (3)$$

where C_{p} is the pressure coefficient, and ρ is the density of the fluid.

Dividing (3) by (1), we obtain

$$\frac{\Delta\bar{p}}{f} = \frac{C_{\mathrm{p}}md}{2St}(\rho u) \quad (4)$$

According to its definition, the mass flow rate in a conduit with cross-sectional area A is

$$q_{\mathrm{m}} = \rho UA \quad (5)$$

Substituting ρU in (5) with (4), it yields

$$q_{\mathrm{m}} = K_{\mathrm{m}}\frac{\Delta\bar{p}}{f} \quad (6)$$

$$K_{\mathrm{m}} = \frac{2A}{md}\cdot\frac{St}{C_{\mathrm{p}}} \quad (7)$$

where K_{m} is the meter coefficient of mass flow rate.

For a specific vortex flowmeter, its geometric parameters are fixed, so the meter coefficient of mass flow rate is only a function of the Strouhal number and the pressure coefficient. Previous study already indicates that the Strouhal number and the pressure coefficient are constant within a wide range of Reynolds numbers [12]. Within that range of Reynolds numbers, the meter coefficient of mass flow rate also keeps constant, which means that the mass flow rate is in direct proportion to the ratio of average pressure drop to vortex shedding frequency. If the vortex shedding frequency and the pressure drop are extracted out of the differential wall pressure, direct mass flow measurement is achieved by a single sensor. Specific values of the meter coefficient of mass flow rate and its applied range of Reynolds numbers need to be determined by experiments.

B. Design of measuring device

The key component of the measuring device of the vortex mass flowmeter is the bluff body. We use a triangular prism as the bluff body. The cross section of the triangular prism is actually a truncated isosceles triangle with its base facing the oncoming fluid, as already shown in Fig.1. The width d of the front face of the bluff body is 7 mm, and the inner diameter D of the measuring conduit is 25 mm. Thereby the blockage ratio b, defined as d/D, is 0.28 for the vortex mass flowmeter developed. The reason for choosing the triangular bluff body is that the two sloped sides of the triangular prism ensure the fluid just behind the front face to decelerate gradually and uniformly, which will induce less oscillation in the course of vortex shedding.

The two pressure tappings are located $1.0D$ upstream and $0.2D$ downstream of the bluff body, respectively. They are connected to a differential pressure sensor with sampling tubes of 2 mm diameter. The effect of the configuration of sampling tubes on the wall pressure measurement was discussed in [14], [15]. According to the estimation of the magnitude and frequency of the output vortex signals, we use a dynamic differential pressure sensor with 0–3.92 kPa measurement range, 1.0 ms response time, and 1.5% accuracy. The sensor and sampling tubes are encapsulated in a protection box on the side of the measuring device. The vortex mass flowmeter developed is given in Fig.2.

Fig.2. The vortex mass flowmeter developed.

C. Design of signal processing and indication

We process the signal output from the pressure sensor with a 32-bit microcontroller STM32. The STM32 series are designed based on the Cortex-M3 CPU, which is of high performance-price ratio and low power consumption. The STM32 used has 72 MHz clock speed, 256 Kbytes of flash memory, and 48 Kbytes of RAM memory. We employ the radix 2 fast Fourier transform (FFT) algorithm to extract the vortex shedding frequency in view of the scarcity of the RAM memory size in the microcontroller. A trigonometric table is prestored in the RAM to reduce the complexity of the calculation further. At the beginning of signal sampling, we use a large sampling frequency to acquire the dynamic feature of the entire signal. When a sampling is completed, the radix 2 FFT algorithm is used to calculate the power spectral density of the signal to obtain the vortex shedding frequency. According to the result, the sampling frequency is altered adaptively to achieve integer-multiple sampling, which can diminish markedly or even eliminate the leakage of power spectrum. The time-averaged value of the signal from the pressure sensor is calculated to represent the pressure drop.

A thin film transistor liquid crystal display (TFT-LCD) is used as the indicator of the vortex mass flowmeter. The TFT-LCD employs another STM32 as its microcontroller. The controller of the TFT-LCD is ILI9320, which receives data from the STM32 via 18-bit data bus and displays them on the screen in the form of signs as well as pictures. An analog resistive film input panel is embedded on the top of the TFT-LCD with the 12-bit ADC controller ADS7843 in charge of human-machine interaction. The communication between the microcontroller and the indicator is Modbus protocol based on RS485 interface. We use ASCII format to transmit data in terms of the requirement for point-to-point communication.

3. EXPERIMENTS

Experiments are performed with air as working fluid at normal ambient temperature and atmospheric pressure. The experimental system primarily consists of a gas pump, a bell prover, the vortex mass flowmeter, and some connecting pipes and control valves, as shown in Fig.3. The bell prover is used as the standard flowmetering device, and it has a volume of 200 L under the working pressure of 2 kPa. The uncertainty of the bell prover is calibrated to be 0.5% with pressure fluctuation less than 50 Pa. The reference mass flow rate provided by the bell prover is

$$q_{mRef} = \rho_a q_v \tag{8}$$

where ρ_a is the density of air deduced from the temperature and pressure in the bell prover, and q_v is the volumetric flow rate calculated by the bell prover's volume change.

The upstream and downstream pipes connecting the vortex mass flowmeter were long enough to ensure vortex shedding fully developed in the flow passage. The flow rate of air was altered by adjusting the control valves.
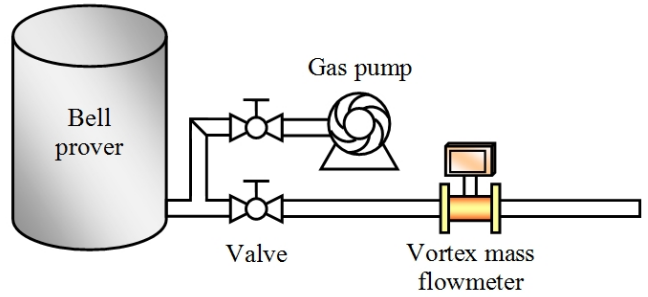

Fig.3. Experimental set-ups.

4. RESULTS & DISCUSSION

To make subsequent analyses more comparable, we define the Reynolds number using the width of the bluff body as the characteristic length:

$$Re = \frac{\rho U d}{\mu} \tag{9}$$

Figs.4–6 show variations of Strouhal number, pressure coefficient, and meter coefficient of mass flow rate, with the Reynolds numbers. Strouhal number, pressure coefficient, and meter coefficient of mass flow rate are calculated by (1), (3), and (7). The variations in Figs.4–6 are characterized by two pronounced phases according to the Reynolds numbers. When Reynolds number is less than 5.5×10^3, the Strouhal number, pressure coefficient, and meter coefficient of mass flow rate possess considerable dispersity and nonlinearity. This irregular behavior is mainly due to the fluid viscosity. It has been found that performance of a vortex flowmeter deteriorates notably at low flow velocity when the influence of fluid viscosity increases [16]. Beyond the critical Reynolds number 5.5×10^3, the Strouhal number, pressure coefficient, and meter coefficient of mass flow rate are nearly constant at an average value of 0.178, 2.177 and 0.0168 m.
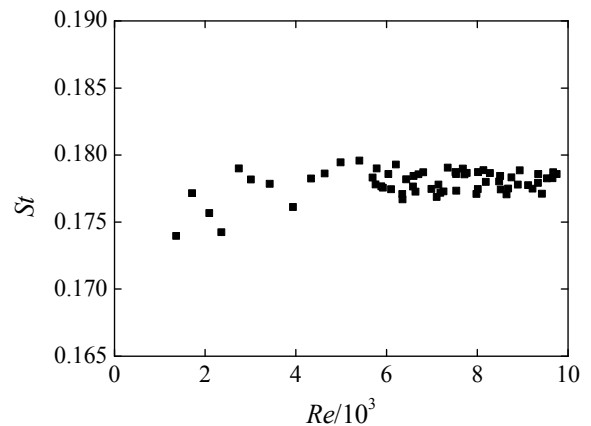

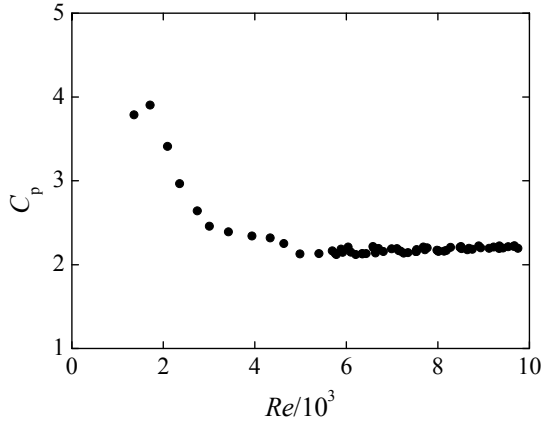Fig.4. Strouhal numbers versus Reynolds numbers.

Fig.5. Pressure coefficients versus Reynolds numbers.
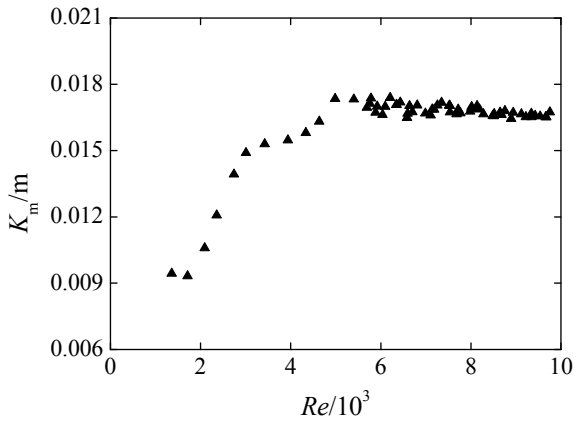

Fig.6. Meter coefficients of mass flow rate with Reynolds numbers.

To extend the measurement range of vortex mass flowmeter at low Reynolds numbers, we introduce a correction factor K_c into (6):

$$q_m = K_c K_m \frac{\Delta \bar{p}}{f} \qquad (10)$$

With this definition, the correction factors are computed at Reynolds numbers ranging from 1.3×10^3 to 5.5×10^3, as shown in Fig.7. A correlation between the correction factor and the Reynolds number is established through polynomial fitting:

$$K_c = -0.0277 \left(\frac{Re}{10^3} \right)^2 + 0.3113 \left(\frac{Re}{10^3} \right) + 0.1478 \qquad (11)$$

whose squared 2-norm R^2 of the residual is 0.9588.

After figuring out and prestoring the meter coefficient of mass flow rate and the correction factors in the EEPROM of the signal processing unit, we take the following feasible steps to obtain the mass flow rate:

a.) Acquire raw sensor signal of vortex mass flowmeter.
b.) Extract vortex shedding frequency and pressure drop from sensor signal.
c.) Compute flow velocity and Reynolds number using (1) and (9).

d.) Choose proper correction factor according to Reynolds number: if Reynolds number is less than 5.5×10^3, then compute correction factor using (11); if Reynolds number is greater than 5.5×10^3, then correction factor is set to 1.
e.) Compute mass flow rate using (10).

On the basis of the measurement results, we calculated the relative errors of the mass flow rates at Reynolds numbers 1.3×10^3 – 9.8×10^3 adopting the above steps, as shown in Fig.8. These errors are basically within $\pm 5\%$, which satisfies most demands of mass flow measurement in engineering. Although compensated by the correction factors, however, the errors at low Reynolds numbers are still fairly large and some even approach 10%. Thereby we should pay special attention to the lower limit of the vortex mass flowmeter.
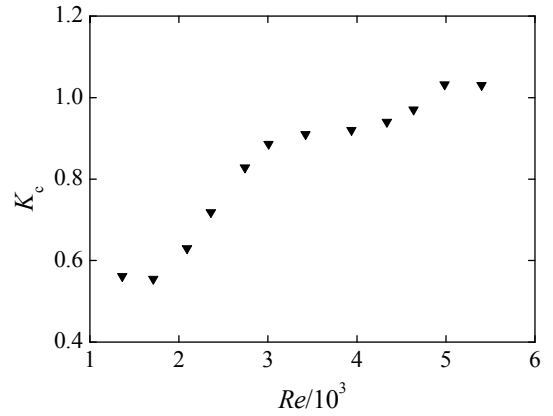

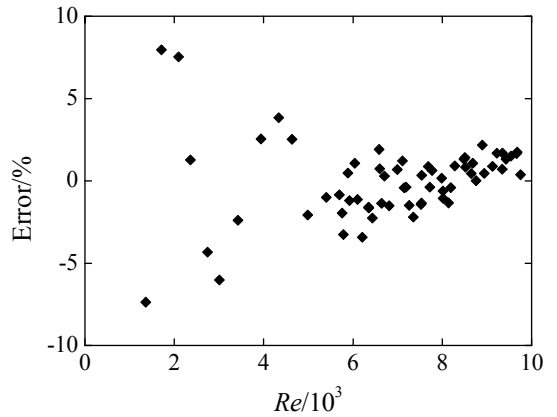Fig.7. Correction factors at low Reynolds numbers.

Fig.8. Measurement errors of vortex mass flowmeter.

5. CONCLUSIONS

In this paper we describe the development of a prototype vortex mass flowmeter with wall pressure measurement. Performance of the vortex mass flowmeter is tested in a bell prover calibration system at Reynolds numbers 1.3×10^3 – 9.8×10^3. On the basis of the measurement results, the meter coefficient of mass flow rate is obtained. It is found that the meter coefficient of mass flow rate is nearly constant at 0.0168 m when Reynolds numbers are greater than 5.5×10^3. Correction factor related to Reynolds numbers is introduced to extend the measurement range of vortex mass flowmeter

at low Reynolds numbers. The relative errors of the vortex mass flowmeter developed are basically within ±5%, which can satisfy most requirements of mass flow measurement in engineering applications.

However, it is also worth noting that the performance of the vortex mass flowmeter may deteriorate notably at low Reynolds numbers due to the fluid viscosity.

ACKNOWLEDGMENT

REFERENCES

[1] Deng, X., Yang, W.Q. (2012). Fusion research of electrical tomography with other sensors for two-phase flow measurement. *Measurement Science Review,* 12 (2), 62-67.

[2] Hall, R. (1990) Measuring mass flow and density with Coriolis meters. *InTech*, 37 (4), 45-46.

[3] Baker, R.C. (2000). *Flow Measurement Handbook.* New York: Cambridge University Press.

[4] Kim, S.D., Lee, H.J., Oh, B.D. (2010). Investigation on application of Parshal flume for flow measurement of low-flow season in Korea. *Measurement Science Review*, 10 (4), 111-115.

[5] Sharma, S.C., Patil, P.P., Vasudev, M.A., Jain, S.C. (2010). Performance evaluation of an indigenously designed copper (U) tube Coriolis mass flow sensors. *Measurement*, 43 (9), 1165-1172.

[6] Pereira, M. (2009). Flow meters: Part 1. *IEEE Instrumentation and Measurement Magazine*, 12 (1), 18-26.

[7] Prasanna, U.R., Umanand, L. (2010). Non-disruptive and null-deflection mass flow measurement by a pressure compensation technique. *Flow Measurement and Instrumentation*, 21 (1), 54-61.

[8] Sun, Z.Q., Zhang, H.J. (2010). Measurement of the flow rate and volume void fraction of gas-liquid bubble flow using a vortex flow meter. *Chemical Engineering Communications*, 197 (2), 145-157.

[9] Venugopal, A., Agrawal, A., Prabhu, S.V. (2011). Review on vortex flowmeter – Designer perspective. *Sensors and Actuators A: Physical*, 170 (1-2), 8-23.

[10] Pankanin, G.L. (2005). The vortex flowmeter: Various methods of investigating phenomena. *Measurement Science and Technology*, 16 (3), R1-R16.

[11] Itoh, I., Ohki, S. (1993). Mass flowmeter detecting fluctuations in lift generated by vortex shedding. *Flow Measurement and Instrumentation*, 4 (4), 215-223.

[12] Zhang, H.J., Huang, Y.M., Sun, Z.Q. (2006). A study of mass flow rate measurement based on the vortex shedding principle. *Flow Measurement and Instrumentation*, 17 (1), 29-38.

[13] Sun, Z.Q. (2010). Mass flow measurement of gas-liquid bubble flow with the combined use of a Venturi tube and a vortex flowmeter. *Measurement Science and Technology*, 21 (5), 055403.

[14] Sun, Z.Q., Zhang, H.J., Zhou, J.M. (2007). Investigation of the pressure probe properties as the sensor in the vortex flowmeter. *Sensors and Actuators A: Physical*, 136 (2), 646-655.

[15] Sun, Z.Q., Zhang, H.J., Zhou, J.M. (2008). Evaluation of uncertainty in a vortex flowmeter measurement. *Measurement*, 41 (4), 349-356.

[16] Goujon-Durand, S. (1995). Linearity of the vortex meter as a function of fluid viscosity. *Flow Measurement and Instrumentation*, 6 (3), 235-238.